Selective Compensation of Voltage Harmonics in a Grid-Connected Microgrid

Savaghebi, M.; Zapata, Josep Maria Guerrero; Jalilian, A.; Vasquez, J.C.; Lee, Tzung-Lin

Published in:
Proceedings of ELECTRIMACS 2011

Publication date:
2011

Document Version
Early version, also known as pre-print

SELECTIVE COMPENSATION OF VOLTAGE HARMONICS IN A GRID-CONNECTED MICROGRID

M. Savaghebi[1], J. M. Guerrero[2,3], A. Jalilian[1], J. C. Vasquez[2], and Tzung-Lin Lee[4]

1. Center of Excellence for Power System Automation and Operation, Iran Univ. of Science and Tech., Iran
2. Department of Automatic Control and Industrial Informatics, Technical University of Catalonia, Spain
3. Department of Energy Technology, Aalborg University, Denmark
4. Department of Electrical Engineering, National Sun Yat-sen University, Taiwan

e-mail: savaghebi@iust.ac.ir

Abstract - In this paper, a method for selective voltage harmonic compensation in a grid-connected microgrid is presented. Harmonic compensation is done through proper control of distributed generators (DGs) interface converters. In order to achieve proper sharing of compensation effort among the DGs, a power named "*Harmonic Distortion Power (HDP)*" is defined. In the proposed method, active and reactive power control loops are considered to control the powers injected by the DGs. Also, a virtual impedance loop and voltage and current proportional-resonant controllers are included. Simulation results show the effectiveness of the proposed method for compensation of voltage harmonics to an acceptable level.

Keywords – Distributed Generator (DG); microgrid (MG); grid-connected; voltage harmonics; selective compensation.

1. INTRODUCTION

Distributed Generators (DGs) may be connected individually to the utility grid or be integrated to form a local grid which is called microgrid (MG). The MG can operate in grid-connected (connected to utility grid) or islanded (isolated from utility grid) modes [1].

DGs often consist of a prime mover connected through an interface converter (e.g. an inverter in case of dc-to-ac conversion) to the ac power distribution system (microgrid or utility grid) [2]. The main role of this inverter is to control active and reactive power injection. In addition, compensation of power quality problems, such as voltage harmonics, can be achieved through proper control strategies.

In [3]-[5], some approaches are presented to use the DG for voltage harmonic compensation. A single-phase DG capable of improving voltage waveform is presented in [3]. For voltage harmonic compensation, DG is controlled to operate as a shunt active power filter. In the other words, DG injects harmonic current to improve voltage waveform.

The approach of [4] is based on making the output voltage of the DG nonsinusoidal in a way that after voltage drop on the distribution line, voltage waveform at the point of common coupling (PCC) becomes sinusoidal. This approach is effective for PCC voltage improvement, but, the negative effect of it on power control of DG is not analyzed.

An interesting approach for compensation of voltage harmonics in an islanded MG is presented in [5]. In this approach, which is implemented in the synchronous (*dq*) reference frame, DGs are controlled to absorb the harmonic current of the load like a shunt active filter. Also, the method of harmonic compensation effort sharing among DGs is presented.

On the other hand, selective voltage harmonic compensation by using shunt active filters is presented in [6]. It is stated in [6] that if the active filter tries to compensate all the harmonics with the same gain, a problem called "*whack-a-mole*" may occur. This problem is the unintentional induction of another harmonic resonance. In order to avoid the problem, in this paper the approach of [5] is modified to achieve selective voltage harmonic compensation in a MG. In addition, by applying a selective compensation method, the capacity of the interface converter may be saved for the main function of the DG (i.e. power injection). Also, the approach of [5] is extended to be used for a grid-connected MG. Furthermore, the method of compensation effort sharing is improved.

In this paper, the overall control system is designed in stationary ($\alpha\beta$) reference frame. The control structure consists of the following loops: active and reactive power controllers, virtual impedance loop, voltage and current controllers, and voltage harmonic compensator.

2. DG INVERTER CONTROL STRATEGY

Fig. 1 shows the power stage of the utility grid and the MG formed by two DGs. The MG consists of a DC prime mover, an inverter, a LC filter for each DG and also an inductor between each DG and load connection point which models the distribution line. As it can be seen in this Fig., a three-phase diode rectifier is considered as the nonlinear load. Also, a static switch is considered to connect the MG to the utility grid (grid-connected operation). In Fig. 1, the resistance R_g and the inductance L_g model the equivalent impedance of the distribution line and the grid-connection transformer.

The proposed control strategy for the DG inverter is also shown in Fig. 1. The details are as following.

2.1. POWER CALCULATION

As it is shown in Fig. 1, $\alpha\beta$ components of the DG output voltage and current are fed to "*Power Calculation*" block. Then, the active and reactive powers at the fundamental frequency (P and Q, respectively) and "*Harmonic Distortion Power (HDP)*" are calculated.

2.1.1. Fundamental Active and Reactive Powers

The instantaneous values of active and reactive powers are calculated as follows [7]:

$$p = v_{c\alpha}\, i_{o\alpha} + v_{c\beta}\, i_{o\beta} \quad (1)$$

$$q = v_{c\beta}\, i_{o\alpha} - v_{c\alpha}\, i_{o\beta} \quad (2)$$

Then, the dc components of p and q (P and Q which are the fundamental active and reactive powers, respectively) are extracted by using two first-order low pass filters with the cut-off frequency of 2Hz.

2.1.2. Harmonic Distortion Power

In this paper, a power named as "*Harmonic Distortion Power (HDP)*" is used for harmonic compensation effort sharing. This power is defined as follows:

$$HDP = 3 * V_{harm,rms} * I_{harm,rms} \quad (3)$$

In equation (3), $V_{harm,rms}$ and $I_{harm,rms}$ are the RMS values of the harmonic (oscillatory) voltage and current, respectively. 5th to 19th order harmonics are used to calculate of RMS values as follows.

$$x_{harm,rms} = \sqrt{\sum_{h=5,7,11,13,17,19} (x_{h,rms}^2)} \quad (4)$$

where $x_{h,rms}$ is the RMS value of h^{th} order voltage or current harmonic.

Thus, for calculation of harmonic distortion power it is necessary to extract harmonic components of DG output current and voltage. In this paper, the components at fundamental and harmonic frequencies are extracted using second-order generalized integrators (SOGI). A SOGI-based bandpass filter (BPF), for extraction of harmonic components with the following transfer function can be achieved as shown in Fig. 2 [8].

$$BPF(s) = \frac{x_{j,h}(s)}{x_j(s)} = \frac{k_h\, \omega_h\, s}{s^2 + k_h\, \omega_h\, s + \omega_h^2} \quad (5)$$

where

- x: voltage or current
- j: represents α or β component
- ω_h: resonant frequency at h^{th} harmonic ($\omega_h = h\omega^*$, in this paper h=1,5,…,19)
- ω^*: reference frequency of the microgrid

k_h: a constant which determines the BPF bandwidth. ($k_1 = \sqrt{2}$ and k_5 to k_{19}= 0.05)

2.2. ACTIVE AND REACTIVE POWERS CONTROL

Assuming a DG which is connected to the electrical network through a mainly inductive distribution line, P and Q are approximately as follows [9], [10]:

$$P = \frac{EV}{X}\phi \quad (6)$$

$$Q = \frac{V}{X}(E - V) \quad (7)$$

where E is the magnitude of the inverter output voltage, V is the network bus voltage magnitude, ϕ is the load angle (the angle between E and V), and X is the distribution line reactance. Assuming zero phase angle for the network voltage, ϕ will be equal to the inverter voltage phase angle.

Thus, P and Q can be controlled by ϕ and E, respectively. According to this, the following droop characteristics [11] are used in this paper:

$$\phi^* = \phi_0 + m_P(P_{ref} - P) + m_I \int (P_{ref} - P) \quad (8)$$

$$E^* = E_0 + n_P(Q_{ref} - Q) + n_I \int (Q_{ref} - Q) \quad (9)$$

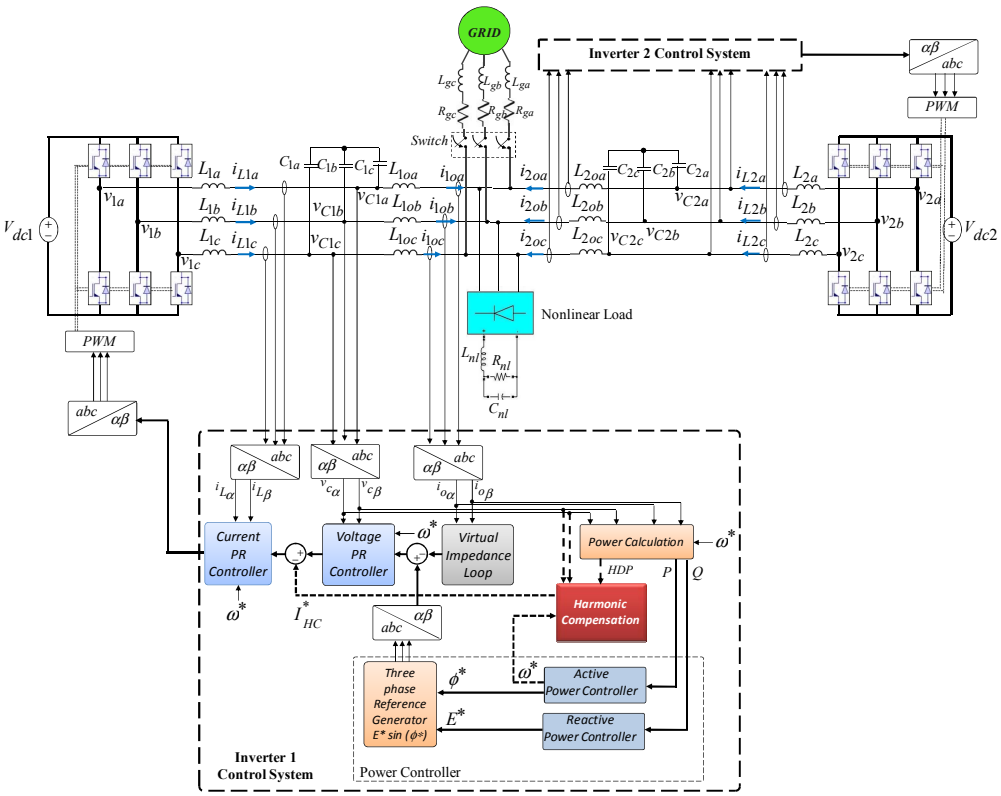

Fig. 1. Power stage and the control system of a MG operating in grid-connected mode.

where

- E^* : voltage amplitude reference
- ϕ^* : phase angle reference
- E_0 : rated voltage amplitude
- ϕ_0 : rated phase angle ($\omega_0 \cdot t$)
- ω_0: rated frequency
- m_P : active power proportional coefficient
- m_I : active power integral coefficient
- n_P : reactive power proportional coefficient
- n_I : reactive power integral coefficient

Now, the design of droop controllers is sufficiently studied in the literature and will not be discussed here. According to [9]-[11] power controllers parameters are selected as listed in Table I.

2.3. Virtual Impedance Loop

Addition of the virtual resistance makes the oscillations of the system more damped [9]. Also, virtual inductance is considered to ensure the decoupling of P and Q. Thus, virtual impedance makes the droop controllers more stable [12]. The virtual impedance can be achieved as shown in Fig.3, where R_v and L_v are the virtual resistance and inductance values, respectively [13].

2.4. Voltage and Current Proportional-Resonant (PR) Controllers

The proportional-resonant (PR) controllers are usually used for the stationary reference frame control [14]. In this paper, voltage and current PR controllers are as (10) and (11), respectively.

$$G_V(s) = k_{pV} + \frac{2k_{rV}\omega_c s}{s^2 + 2\omega_c s + (\omega^*)^2} \tag{10}$$

$$G_I(s) = k_{pI} + \frac{k_{rI1}\, s}{s^2 + (\omega^*)^2} + \frac{k_{rI5}\, s}{s^2 + (5\omega^*)^2} + \frac{k_{rI7}\, s}{s^2 + (7\omega^*)^2} \tag{11}$$

where

- k_{pV} : voltage proportional coefficient
- k_{rV} : voltage resonant coefficient
- ω_c : voltage cut-off frequency
- k_{pI} : current proportional coefficient
- k_{rI1} : current resonant coefficient at fundamental frequency

- k_{rI5}: current resonant coefficient at 5th harmonic
- k_{rI7}: current resonant coefficient at 7th harmonic

As shown in Fig. 1, the voltage controller follows the mainly fundamental frequency reference which is generated by the virtual impedance loop and the droop characteristics. So, only the fundamental frequency resonant controller is considered. Also, to provide more stability, the resonant part is considered as a BPF [15].

Also, since the "*Harmonic Compensation*" block output contains 5th and 7th harmonic components (as described in the next Subsection), the resonant parts for these harmonics are included in the current controller.

Considering the parameters listed in Table II, the Bode diagrams of voltage and current controllers are as Figs. 4(a) and 4(b), respectively. As shown, current controller provides very high gains at 1st (fundamental), 5th, and 7th harmonics which ensure zero steady-state error. Also, voltage controller has a wider resonant peak, therefore is less sensitive to frequency fluctuations. The gain at resonant frequency is limited, however, still high enough to ensure a small tracking error.

As shown in Fig. 1, the output of the current controller is transformed back to the *abc* frame to provide the reference voltage for the pulse width modulator (*PWM*). Finally, the *PWM* block controls the switching of the DG inverter.

2.5. Selective Compensation of Voltage Harmonics

In this Subsection, the harmonic compensation method of [5] is modified to provide selective harmonic compensation. Also, an improved method for compensation effort sharing is proposed.

The details of "*Harmonic Compensation*" block of Fig. 1 are shown in Fig. 5. As seen, at first, h^{th} harmonic component of the DG output (capacitor) voltage ($v_{\alpha\beta,h}$) is extracted using a SOGI-based BPF (Fig. 2). On the other hand, *HPD* is multiplied by a constant which is called "*Harmonic Compensation Gain (HCG)*" to generate "*Harmonic Conductance Command (G*)*". Thus, the amount of compensation is proportional to *HDP* and *HCG*. Proper selection of *HCG* ensures that compensation will not lead to DG inverter overloading or control system instability. Then, $v_{\alpha\beta,h}$ and *G** are multiplied to generate h^{th} harmonic compensation reference current ($I^*_{HC,h}$). In this way, *G** makes the DG behave as a resistance at harmonic frequencies to damp the voltage harmonics. Finally, the references of different harmonics are added together to generate the total reference for the compensation (I^*_{HC}).

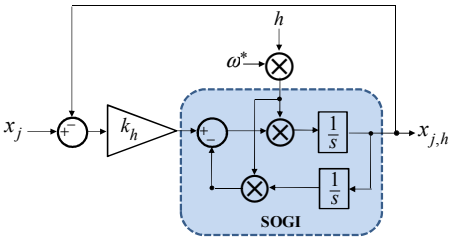

Fig. 2. SOGI-based BPF block diagram.

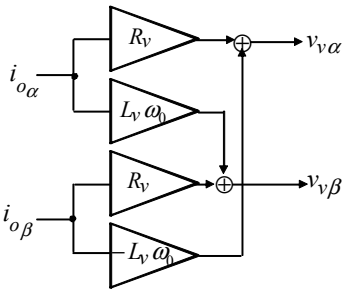

Fig. 3. Virtual impedance block diagram.

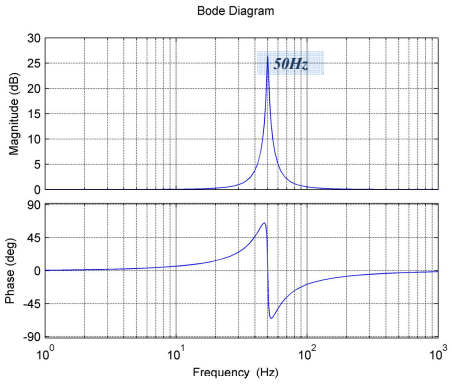

(a)

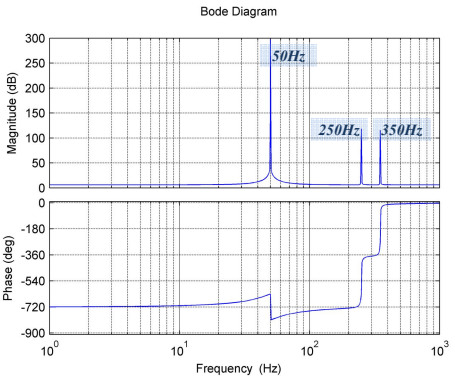

(b)

Fig. 4: Bode diagrams
(a) voltage controller (b) current controller

As a result of compensation, *HDP* will decrease (See the next Section). So, an inherent negative feedback exists in this compensation method. This is like a droop characteristics which helps to achieve sharing of compensation effort.

On the other hand, in [5] a power named "*Harmonic Volt-Ampere Reactive (H)*" is used for sharing of harmonic compensation effort among the DGs. With compensation of voltage harmonics this power increases. So, in order to achieve the sharing of compensation effort, the following droop characteristic is presented in [5].

$$G^* = G_0 + HCG(H_0 - H) \qquad (12)$$

In (12), H_0 and G_0 are the rated values of harmonic VAr and conductance, respectively.

The method presented in [5] for estimation of H_0 is not straight-forward. On the other hand, if $H>H_0$ the control system becomes instable. Also, inclusion of G_0 in (12) is not justified. In the present paper, these problems are solved through considering *HDP* instead of *H* for sharing of harmonic compensation effort.

3. Simulation Results

Simulation studies are performed on the electrical system of Fig. 1. The MG and the utility grid are rated at 400V/50Hz. Power stage parameters are shown in Table III (the subscripts *a*, *b* and *c* are not shown). In order to simulate asymmetrical distribution lines, $L_{1o}=L_o/2$ and $L_{2o}=L_o$. The switching frequency of the DGs inverter is 10 kHz.

R_v and L_v are chosen as 1Ω and 2mH, respectively. Also, *HCG* is set to 0.04 and harmonic compensation is activated at t=0.7 sec.

Fig. 6 shows *P* and *Q* values of the DGs. P_{ref} and Q_{ref} are set to 1500W and 0VAr, respectively. It can be seen that the reference values are tracked-well and the well-tracking is maintained after harmonic compensation activation. Active and reactive powers supplied by the utility grid (P_g and Q_g, respectively) are shown in Fig. 7.

The DGs output voltage improvement due to compensation is obvious in Fig. 8. As seen, DG1 voltage is more distorted since the line impedance between DG1 and nonlinear connection point is lower. DGs voltage *THD* and *HDP* are depicted in Figs. 9(a) and 9(b), respectively. As shown, *THD* and *HDP* are both reduced due to compensation. The reduction of 5th and 7th voltage harmonics of DG1 can be seen in Fig. 10. Harmonics of DG2 voltage has the same behavior.

I. Power controllers parameters

E_0	ω_0	m_P	m_I	n_P	n_I
$230\sqrt{2}$	100*pi	0.0002	0.002	0.01	0.3

I. PR controllers parameters

k_{pV}	k_{rV}	ω_c	k_{pI}	k_{rI1}	k_{rI5}	k_{rI7}
1	20	4	2	500	90	90

IIII. Electrical system parameters

V_{dc} (V)	L (mH)	C (μF)	L_o (mH)	R_{nl} (Ω)	L_{nl} (mH)	C_{nl} (μF)	R_g (Ω)	L_g (mH)
650	1.8	25	1.8	25	0.084	235	1	10

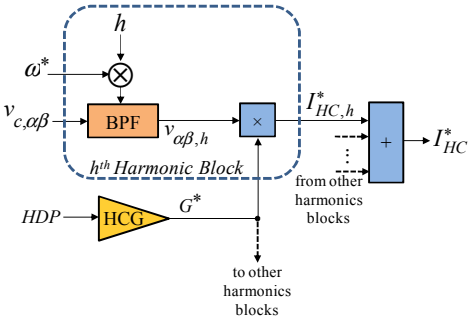

Fig. 5. Selective harmonic compensation method.

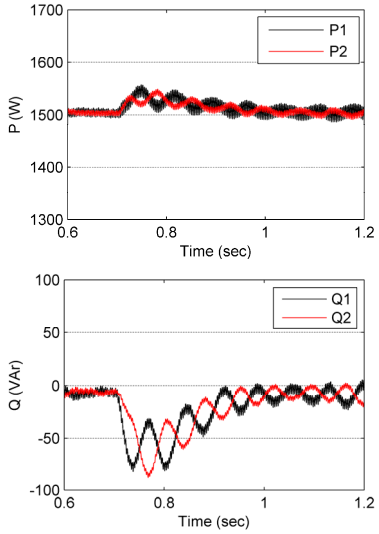

Fig. 6. DGs active and reactive powers.

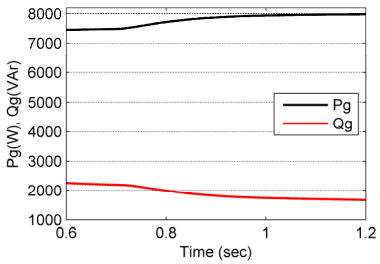

Fig. 7. Utility grid active and reactive powers.

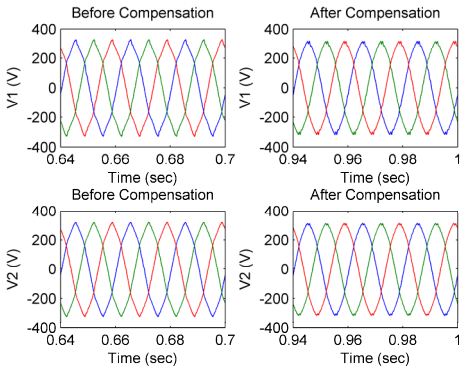

Fig. 8. DGs output voltage.

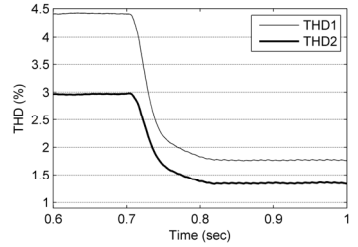

(a)

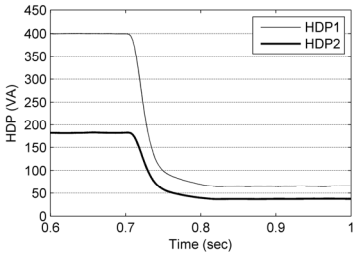

(b)

Fig. 9. (a) *THD* (b) *HDP*

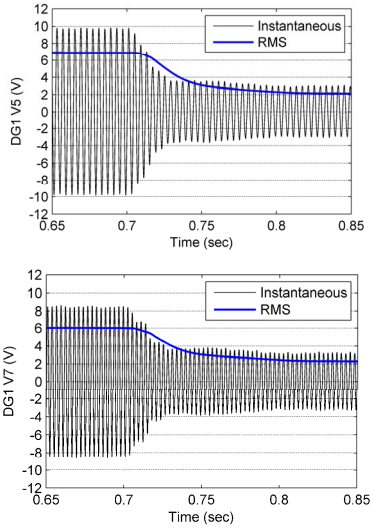

Fig. 10. 5th and 7th voltage harmonics of DG1

4. CONCLUSIONS

In this paper, an approach for selective compensation of voltage harmonics in a microgrid is presented. In order to improve harmonic compensation effort sharing, a new definition for harmonic power is used. The results show that by using the proposed control approach fundamental and distortion powers are properly shared between DGs and also the selected harmonics (5th and 7th) are well compensated. Furthermore, the *THD* values of the DGs output voltage are decreased.

5. REFERENCES

[1] S. B. Patra, "Techniques for developing reliability-oriented optimal microgrid architectures," PhD. Diss., New Mexico State University, May 2007.

[2] S. Porkar, A. Abbaspour-Tehrani, and S. Saadate, "An approach to distribution system planning by implementing distributed generation in a deregulated electricity market," Pow. Eng. Large Eng. Sys. Conf., Oct. 2007.

[3] M. Cirrincione, M. Pucci, and G. Vitale, "A single-phase DG generation unit with shunt active power filter capability by adaptive neural filtering," IEEE Trans. Ind. Elec., vol. 55, no. 5, pp. 2093-2110, May 2008.

[4] H. Patel, and V. Agarwal, "Control of a stand-alone inverter-based distributed generation source for voltage regulation and harmonic compensation," IEEE Trans. Pow. Del., vol. 23, no. 2, pp. 1113-1120, Apr. 2008.

[5] T. L. Lee, and P. T. Cheng, "Design of a new cooperative harmonic filtering strategy for distributed generation interface converters in an islanding network," IEEE Trans. Pow. Elec., vol. 22, no. 5, pp. 1919-1927, Sept. 2007.

[6] T. L. Lee, J. C. Li, and P. T. Cheng, "Discrete frequency tuning active filter for power system harmonics," IEEE Trans. Pow. Elec., vol. 24, no. 5, pp. 1209-1217, May 2009.

[7] H. Akagi, Y. Kanagawa, and A. Nabase, "Instantaneous reactive power compensator comprising switching devices without energy storage components," IEEE Trans. Ind. App., vol. IA-20, no. 3, p. 625, May/Jun. 1984.

[8] M. Ciobotaru, R. Teodorescu, and F. Blaabjerg, "A new single-phase PLL structure based on second order generalized integrator," Pow. Elec. Specialists Conf. (PESC), Oct. 2006.

[9] J. M. Guerrero, J. Matas and L. G. de Vicuña, M. Castilla and J. Miret, "Decentralized control for parallel operation of distributed generation inverters using resistive output impedance," IEEE Trans. Ind. Elec., vol. 54, no. 2, pp. 994-1004, Apr. 2007.

[10] E. Barklund, N. Pogaku, M. Prodanovic´, C. Hernandez-Aramburo and T. C. Green, "Energy management in autonomous microgrid using stability-constrained droop control of inverters," IEEE Trans. Pow. Elec., vol. 23, no. 5, pp. 2346-2352, Sept. 2008.

[11] Y. Li, D. M. Vilathgamuwa, and P. C. Loh, "Design, analysis, and real-time testing of a controller for multibus microgrid system," IEEE Trans. Pow. Elec., vol. 19, no. 5, pp. 1195-1204, Sept. 2004.

[12] J. M. Guerrero, L. G. Vicuna, J. Matas, M. Castilla, and J. Miret, "Output impedance design of parallel-connected UPS inverters with wireless load sharing control," IEEE Trans. Ind. Elec., vol. 52, no. 4, pp. 1126-1135, Aug. 2005.

[13] Y. W. Li and C. N. Kao, "An accurate power control strategy for inverter based distributed generation units operating in a low voltage microgrid," Energy Conv. Cong. and Exp. (ECCE), 2009.

[14] F. Blaabjerg, R. Teodorescu, M. Liserre and A. V. Timbus, "Overview of control and grid synchronization for distributed power generation systems," IEEE Trans. Ind. Elec., vol. 53, no. 5, pp. 1398-1409, Oct. 2006.

[15] Y. Li, D. M. Vilathgamuwa, and P. C. Loh, "Microgrid power quality enhancement using a three-phase four-wire grid-interfacing compensator", IEEE Trans. Ind. Appli., vol. 41, no. 6, pp. 1707-1719, Nov./Dec. 2005.